

EIT DEM TOOL User's Guide
John Cook
Jeffrey Newmark
Naval Research Laboratory

Introduction

The Solar and Heliospheric Observatory (SOHO) spacecraft carries onboard the Extreme-ultraviolet Imaging Telescope (EIT), which images the Sun in a field-of-view extending out to 1.4 R_{\odot} in four wavelength channels covering a temperature range from 80,000 K to 2.5×10^6 K (Delaboudiniere et al. 1995). The 1024x1024 CCD detector has a spatial resolution of two pixels, where 1 pixel subtends 2.6 arcsec. The SOHO spacecraft was launched in December 1995, and scientific observations began in January 1996.

Cook, Newmark, and Moses (1999) have developed a technique to calculate the differential emission measure (DEM) using images from the four wavelength channels of the EIT instrument at 171 Å, 195 Å, 284 Å, and 304 Å. An individual DEM curve, covering the temperature range from $\log T = 4.6$ to 6.5 in 0.1 dex steps, is constructed for each pixel in the EIT field-of-view. We call the result a DEM map. The DEM map is determined so as to best match the original four EIT images when synthetic EIT images are back-calculated from it. This technique uses the CHIANTI program (Dere et al. 1997) as the atomic physics engine for its calculations.

We have placed the computer programs that produce the DEM maps, all in the IDL programming language, in the Solar Soft collection of software products. The programs should be run in a home IDL environment with paths set to Solar Soft, including the CHIANTI package. In this User's Guide we briefly describe the construction technique, illustrate the use of the DEM tool with examples for running it, and finally present a more detailed discussion of a sample application of the DEM tool to model solar EUV irradiances, where we also discuss some further aspects of our basic DEM tool technique in greater detail.

For further help and coaching with using our DEM tool for EIT, contact Jeff Newmark at jeffrey.newmark@nasa.gov.

Basic idea of the DEM construction

The differential emission measure (DEM) provides a compact summary of the solar atmospheric density and temperature structure along an individual line-of-sight, determined from emission line intensities. The intensity of an optically thin emission line (in a simple 1-D form for this discussion) is found from

$$\begin{aligned} I(\text{ergs cm}^{-2} \text{ s}^{-1} \text{ sr}^{-1}) &= (1/4\pi)(hc/\lambda)N_{upper}A_{ul} \\ &= (1/4\pi)(hc/\lambda)N_e(N_H/N_e)(N_{el}/N_H)(N_{ion}/N_{el})(N_{upper}/N_{ion})A_{ul} \\ &= (1/4\pi)(hc/\lambda)0.8A_{el}A_{ul} \int_{\log T} R_{ion}(N_{upper}/N_{ion}N_e)(N_e^2 d\ell/d \log T) d \log T , \end{aligned}$$

where N_{upper} is the population of the upper level of the transition, A_{ul} is the radiative rate from the upper to lower level, ℓ is the line of sight, (N_H/N_e) is 0.8 for a completely ionized plasma with solar abundances, (N_{el}/N_H) is the elemental abundance A_{el} , (N_{ion}/N_{el}) is the ionization balance R_{ion} , and $N_e^2 d\ell/d \log T$ is the logarithmic differential emission measure in the line-of-sight. N_{upper}/N_{ion} is found from the atomic level population statistical equilibrium equations. For allowed lines, or for forbidden lines in an electron density range where they still behave as allowed lines, the quantity $(N_{upper}/N_{ion}N_e)$ is almost constant with N_e if only collisions and radiative transitions need be considered, and intensity is directly proportional to the DEM. The integrand is sharply peaked at a temperature which can be called the temperature-of-formation of the emission.

We have developed a technique to calculate the differential emission measure using images from the four wavelength channels of the EIT instrument at 171 Å, 195 Å, 284 Å, and 304 Å. We use the elemental abundances of Feldman et al. (1992), and the ionization balances of Mazzotta et al. (1998) in calculating intensities.

The EIT images when processed by `eit_prep` are in instrument intensity units DN s^{-1} . From a given DEM curve the unique synthetic instrument units intensity for each channel can be found by calculating the absolute intensity spectrum over the EIT wavelengths from the DEM curve and then applying the instrument efficiency function. You can't go the other way, from an individual channel instrument units intensity to a unique DEM curve, because different DEM curves can produce the same synthetic instrument units intensity. But looking for a single DEM curve that simultaneously reproduces all four channel instrument units intensities is more constrained. Once you obtain that DEM curve you can calculate model absolute intensities.

We begin with a standard initial starting DEM curve (the CHIANTI active region DEM, although our method does not depend on the exact starter choice), which produces starting synthetic absolute intensity spectra over each EIT channel. From these synthetic spectra, synthetic EIT channel intensities are found. We then use the observed EIT image intensities (DN s^{-1}) in all four channels to modify the initial DEM to produce individual DEM curves for each pixel that will best reproduce the observed DN s^{-1} intensities, giving a DEM map of the entire field-of-view. Our DEM map is an individual DEM curve for each pixel of an image, covering

the temperature range $\log T = 4.6$ to 6.5 in 0.1 dex steps.

The intensity is linear with DEM for emission lines which are emitting in their allowed range of electron density. The EIT channel passbands contain a number of forbidden lines, and we first checked to see if their intensity contributions make the total passband intensities significantly pressure-sensitive over a range of representative solar electron pressures, which they were not. Using the initial starting DEM curve and its calculated four synthetic EIT channel intensities, we determine for each individual pixel the scaling constants for each of the four channels which would multiply the starting DEM to best reproduce the four observed EIT intensities. Naturally, the four scaling constants are almost never identical: simply linearly increasing or decreasing the initial active region DEM curve will not reproduce the four intensities simultaneously. The actual shape of the initial DEM curve must be modified. From the response curves with temperature for each channel, we identified the temperatures of peak response (temperature-of-formation). We generate a scaling function vs. $\log T$ from the four individual channel scaling constants placed at their peak response temperatures, interpolated over the $\log T$ grid. We then multiply the initial DEM curve by the scaling values over the temperature grid, resulting in an individualized DEM curve which now better reproduces the four observed EIT intensities. Finally, we iterate once using this new, now individualized DEM map as the starting DEM for each pixel to obtain a final DEM map. We found no further improvement iterating more than once. The actual technique is slightly more complex because we must handle explicitly the presence of significant multiple temperature response peaks in the 304 \AA (three peaks which must be considered) and 284 \AA (two peaks) channels, and we do some careful bookkeeping of the multiple temperature contributions to these last two channels in calculating the synthetic intensities and scaling constants.

The He II 304 \AA line is difficult to model, but is critical to include in the DEM map construction as part of the total EIT 304 \AA channel intensity, which controls the cooler end of the DEM curve. This line is inherently optically thick and so not appropriate for a direct DEM approach to calculating its intensity. It is also anomalous from other, optically thin, transition region lines in that it clearly shows coronal holes. The DEM map construction uses an empirical correction factor for the direct He II 304 \AA intensity calculated by the CHIANTI atomic physics engine for an optically thin plasma. Cook, Newmark, and Moses (1999) obtained this scaling factor from examining a collection of observed He II 304 \AA intensity values for quiet and active regions. The EIT 304 \AA channel contains contributions from cooler transition region plasmas emitting the He II 304 \AA line, as well as from hotter coronal plasmas emitting in the same wavelength range. The hotter contribution must be consistent with the DEM curve well-determined by the three other coronal EIT channels, and the required consistency in the final DEM to reproduce all four EIT channels does help to check the empirical He II scale factor, which we believe to be reasonable. But again, this is inherently a difficult line to model theoretically.

From these DEM maps we can calculate a synthetic solar image for any emission line, wavelength interval, or instrumental passband with measured (or assumed) passband efficiencies. In addition we can calculate a synthetic full disk irradiance from the synthetic solar image. Because the EIT images and the resulting DEM maps extend off-disk, these calculated irradiances include the irradiance contribution from off-disk, which can be significant in the EUV wavelength range.

Running the DEM tool in IDL

We assume that the user is familiar with IDL. In this section we list the initial comments sections of the two IDL procedures employed, and give examples of program parameter choices to perform various tasks using the DEM tool. The basic driver procedure is EIT_DEM_TOOL. It defines internally two IDL functions and a separate IDL procedure called EIT_KCORR, which computes the scaling factors to modify the shape of the initial DEM curve. EIT_DEM_TOOL calls a separate IDL function EIT_LINE_MAP, whose comments section is listed after EIT_DEM_TOOL.

```
;+
; NAME:
;   EIT_DEM_TOOL
;
; A user guide is included in the Solar Software distribution. For further information
; go to your local directory $SSW/soho/eit/idl/response/dem_tool/user_guide.pdf
;
;
; PURPOSE:
;   Create a Differential Emission Measure (DEM) Map, i.e. computed for
;   each pixel individually, based upon the 4 EIT channels. Optionally,
;   also returns a line/bandpass map or the irradiance for chosen line.
;   DEM maps can be from pre-computed daily map database
;
; CATEGORY:
;   Analysis
;
; CALLING SEQUENCE:
;   eit_dem_tool,files,dem_map,temp,[mk_line=mk_line],[line_map=line_map],$
;   [wmin=wmin],[wmax=wmax],[irradiance=irradiance],$
;   [no_dem_map=no_dem_map],[date = date],[leak_284=leak_284],$
;   [coefs_only=coefs_only],[nrl=nrl]
;
; INPUTS:
;   files          - Names of 4 EIT raw files in order 171,195,284,304
;                  or a processed (1024,1024,4) array
;
; OPTIONAL INPUT KEYWORD PARAMETERS:
;   mk_line       - set to produce output line map
;   ion           - set to ion name for line maps
;   wmin          - minimum wavelength to consider for line maps
;   wmax          - maximum wavelength to consider for line maps
;   irradiance    - set if only want line irradiance
;   no_dem_map    - set if do not wish calculation of output DEM
;                  map i.e. only wish line_map output
;   date          - read in pre-computed DEM for set date
;   leak_284      - set to use in eit_prep for the 284 A channel light leak
;   coefs_only    - set if return correction coefficients only
```

```

;   nrl           - REQUIRED to set for FITS files from NRL archive (to run the
;                 NRL version of eit_prep)
;
;
; OUTPUTS:
;   dem_map      - differential emission measure map at
;                 26 predefined temperatures logT = 4.0 – 6.5, step 0.1
;   temp         - temperatures (log)
;
; OPTIONAL OUTPUT KEYWORD PARAMETERS:
;   LINE_MAP     - output line map or irradiance
;
; COMMON BLOCKS: none.
;
; SIDE EFFECTS:
;
; RESTRICTIONS:
;
; PROCEDURE:
;   Modifies starter DEM to fit observed EIT data.
;   Starter DEM = CHIANTI V3 active_region for logT = 4.6 - 6.5 and
;   CHIANTI V5 quiet_sun for logT = 4.0 - 4.6
;
; SUBROUTINES:
;   E_INTERP, E_FIT2, EIT_KCORR : included in this file, automatically compiled
;   EIT_LINE_MAP : Separate procedure
;   MK_EIT_SPEC: Included in EIT_LINE_MAP
;
; MODIFICATION HISTORY:
;   Written by: J. Newmark      October 2001
;   Modified:  J. Newmark      May 2006
;               N. Rich        October 2010 Add /NRL keyword
;
;-

```

The IDL function `EIT_LINE_MAP` is called from `EIT_DEM_TOOL`, and itself includes a subroutine procedure `MK_EIT_SPEC` which uses the `CHIANTI` package to perform the atomic physics calculations.

```

;+
; NAME:
;   EIT_LINE_MAP
;
; PURPOSE:
;   Create a line/bandpass map based upon input differential emission
;   measure (DEM) for EIT like instrument.
;
; CATEGORY:

```

```

; Analysis
;
; CALLING SEQUENCE:
;   line_map =eit_line_map(wave,dem,intemp,x,coefs,ion=ion,wmin=wmin,$
;   wmax=wmax,he_fac=he_fac,trange=trange,instr=instr,$
;   irradiance=irradiance,delta_wave=delta_wave, $
;   xyidx=xyidx,nocon=nocon,abund=abund, $
;   eqion=eqion,pressure=pressure)
;
; INPUTS:
;   wave           - EIT bandpass or particular line wavelength
;   dem            - input DEM (1D or 3D)
;   intemp         - temperature array (1D) corresponding to DEM
;   x              - EIT specific line parameter
;
; OPTIONAL INPUT KEYWORD PARAMETERS:
;   coefs          - coefficients to "tweak" input DEM
;   ion            - choice of output line if using single line
;   wmin           - minimum wavelength to consider for line maps
;   wmax           - maximum wavelength to consider for line maps
;   he_fac         - enhance factor for Helium II 304 over default
;                   spectrum
;   trange         - array of temperature indices to consider if not
;                   full range
;   instr          - set to particular instrument, default = 'eit'
;                   set to 'dum' or anything else for simple lines
;   irradiance     - set if only want line irradiance
;   delta_wave     - wavelength bin size for subsetting wavelength
;                   range. Default is 1 bin for wmin->wmax. Only
;                   useable with irradiance keyword
;   xyidx         - Index values of array that should be used. All
;                   others are set to zero
;   nocon          - Set if do not want continuum included in calculation
;   pressure       - Set if want spectra calculated with specific Pressure,
;                   default = 1.0E+15
;   abund         - Set if want spectra calculated with specific Abundance,
;                   default = Coronal (Feldman) et al.
;   eqion         - Set if want spectra calculated with specific ionization
;                   equilibrium, default = Mazzotta et al. ext
;
; OUTPUTS:
;   line_map       - computed line/bandpass map
;
; OPTIONAL OUTPUT KEYWORD PARAMETERS:
;
; COMMON BLOCKS: none.
;
; SIDE EFFECTS:
;
; RESTRICTIONS:

```

```

; Requires Pre-computed spectra using CHIANTI Isothermal procedure
;
; PROCEDURE:
;
; SUBROUTINES: Include MK_EIT_SPEC for computing Isothermal spectra
;
; Helium enhancement = 9.5 Any change in the elemental abundances
;                           employed from our Feldman default would
;                           require re-examination of the Helium
;                           enhancement factor
;
;
;
;
; MODIFICATION HISTORY:
;   Written by: J. Newmark      October 2001
;   Modified:  J. Newmark      May 2006
;   Modified:  J. Newmark      July 2010
;-

```

We strongly suggest that these programs be run using the standard default choices of atomic parameters. Unless the user is prepared for significant work in understanding the code and time in testing and verifying any results with alternative parameter choices, they are best avoided. In particular, the He II 304 Å emission line is a special problem, and the parameter `he_fac` is chosen for the particular elemental abundance choice we employ. We have retained several features which we introduced for special calculations, and that have been left in the code but will not be described in this guide. Be warned. An example is the `nocon` keyword. We include the CHIANTI continuum calculation as the default setting, and advise you to also. We in past checked the continuum contribution to the total by comparing the `nocon = 0` and `nocon = 1` calculations, and leave this keyword in. For special calculations we often changed code instead of adding general keywords, and to do some special calculations you too will have to slightly edit the code.

The most direct use of our DEM tool is to produce emission measure maps of the differential emission measure $N_e^2 dl/dT$ (this is the type of the CHIANTI reference DEMs). In addition, the output array `dem_map` gives the log DEM values. However, for most purposes we find that the logarithmic DEM, $N_e^2 dl/d \log T$ in units cm^{-5} , is more useful, and this is what we will always mean by DEM. This DEM is just $\log_{e10} T N_e^2 dl/dT$, and its log is `dem_map(i,j,*)+temp(*)+0.3622`, where the output vector `temp` is `logT`. The default temperature range of `temp` is nominally `logT = 4.0 – 6.5 dex`, in 0.1 dex steps. The `temp` output vector will have 26 elements. The first six of these, `temp(0:5)`, are for a highly schematic cool scaled quiet Sun downward extension of the DEM smoothly joining at `logT=4.6`, which we added to get some representation of cool continua when we were investigating modeling of possible wavelength coverage to higher wavelengths than 550 Å. The `dem_map` output array is nominally of dimension (1024,1024,26), the EIT 1024x1024 field-of-view at 26 temperatures. The individualized DEM curve calculation is only performed over `logT = 4.6 – 6.5`, the temperature range actually sampled by the four EIT channels. We suggest that the user simply ignore the DEM output below `logT = 4.6`, `dem_map(1024,1024,0:5)`, unless willing to perform significant checking and verification.

You must keep in mind the difference between temperature and wavelength dependencies. The temperature range sampled by EIT sets the temperature range coverage of the DEM maps. But any optically thin emission from whatever wavelength that is actually formed in this temperature range can be modeled, such as the Fe XIV 5303 Å coronal green line, if CHIANTI can compute the atomic level populations. Solar flare lines cannot be treated, nor can hotter (temperature-of-formation $> \log T = 6.5$) active region emissions; nor can cooler ($< \log T = 4.6$) emissions be accurately treated at any wavelength. We have checked carefully the DEM calculations over the default wavelength range 165-550 Å, and verified that broadband intensities produced from the DEM maps are reasonable (“broadband” because there are some weak cooler and hotter lines in the range that won't be accurately modeled, but they don't significantly contribute over, say, 10 Å intervals anywhere in this wavelength range). Read the final section for further discussion.

The raw (or processed; see keywords list) EIT data must be input in `eit_dem_tool`. The easiest procedure is to put the four raw files in the working IDL directory, but at least include the full path name to the data if you store it in a separate directory.

To produce the basic dem map, simply run

```
eit_dem_tool,['filename1','filename2','filename3','filename4'],dem_map, temp
```

The input files must be in the order: 171 Å, 195 Å, 284 Å, 304 Å channel filenames.

Each time `eit_dem_tool` is run, the function `eit_line_map` looks for an IDL `.save` file usually named `radiance_unit_dem_con.save` in the working directory, which contains information calculated using CHIANTI necessary to the DEM map construction. If this file is not present in the directory, such as the first time run, it is calculated and the `.save` file is stored. The next time `eit_dem_tool` is run it does not have to repeat these calculations but simply restores the `.save` file. If you later want to do a new calculation with new parameter and keyword choices, make sure to delete the old `.save` file so that a new one based on your current choices is calculated.

The IDL function `eit_line_map` is used in two modes. It is called from `eit_dem_tool` in forming the DEM map output, when it returns synthetic values for DN s^{-1} in each EIT channel from the DEM map being constructed. It also is used to make `line_map`, which is in absolute intensity units, when `mk_line` is set in `eit_dem_tool`.

To make a line intensity or broadband map (or the scalar line irradiance if the irradiance keyword is set), set the `mk_line` and `line_map` keywords. The output intensity array `line_map(1024,1024)` is an array of intensities in units $\text{ergs cm}^{-2} \text{s}^{-1} \text{sr}^{-1}$ (the irradiance scalar is $\text{ergs cm}^{-2} \text{s}^{-1}$). The keywords `wmin` and `wmax` are used to define the wavelength interval summed over. In `eit_line_map` an additional `.save` file analogous to `radiance_unit_dem_con.save` should be calculated over a narrower wavelength range around the line or wavelength band, but at a higher wavelength resolution than the default 1 Å over the 165–550 Å range, typically over an angstrom or two with 0.02 Å resolution. We have coded in examples for three emission lines, but you will need to edit (described next) for other lines. The CHIANTI line list can be consulted to verify what wavelength CHIANTI assigns and what other lines are nearby. For a new line or interval not calculated previously, explore several choices of `wmin` and `wmax` and the wavelength choices in the call to `isothermal` (again, described next) to satisfy yourself that the output

intensity map is not sensitive to the exact values used (contains the core wavelength assigned by CHIANTI, does not include any nearby possible blends of same element and ionization stage).

We give an example for the Fe XIV 5303 Å coronal green line. You can run

```
eit_dem_tool,[4 filenames as before],dem_map,temp,/mk_line,line_map=fe14_map,  
ion='fe14',wmin=5304,wmax=5305
```

Before this, you may need to edit eit_line_map in the subsection defining mk_eit_spec that runs the CHIANTI isothermal procedure. Make a copy in your working directory to edit. Look at

if keyword_set(ion) then begin

```
; Here are three sample line calculations for He II 304 A, Si XI 303 A, Fe XIV 5303 A  
; If you want another line, add new code appropriate for new line; keyword sngl in  
; isothermal call of format element_ionization stage  
isothermal,303.,304.,.02,temp,waves,spec0,presure=pressure,/noverbose,cont=cont,$  
  sngl='he_2',abund=abund,ioneq=eqion  
save,file='he2_radiance_unit_dem_'+app+'.save',temp,presure,spec0,waves  
  
isothermal,303.,304.,.02,temp,waves,spec0,presure=pressure,/noverbose,cont=cont,$  
  sngl='si_11',abund=abund,ioneq=eqion  
save,file='si11_radiance_unit_dem_'+app+'.save',temp,presure,spec0,waves  
  
isothermal,5304,5305,.02,temp,waves,spec0,presure=pressure,/noverbose,cont=cont,$  
  sngl='fe_14',abund=abund,ioneq=eqion  
save,file='fe14_radiance_unit_dem_'+app+'.save',temp,presure,spec0,waves
```

Notice that we have coded examples for three lines. No edit is necessary for these, but other lines will need to be coded. Then re-compile explicitly in IDL with “.run eit_line_map”. The first time you run with ion set, the three .save files for fe14, si11, and he2 (and broadband, below) will appear in your working directory. In choosing the isothermal wavelength range and resolution, what matters is where CHIANTI has assigned the wavelength (Fe XIV 5304.57; Si XI 303.33, He II 303.78). Do not set wmin or wmax outside the range used in the isothermal call. Notice in the code that if you set ion='he2' the CHIANTI optically thin intensity will be scaled by he_fac.

We also illustrate a broadband example, for the intensity over 300-310 Å (all the emissions, with the He II 304 Å emission line the strongest component). The call is

```
eit_dem_tool,[4 filenames as before],dem_map,temp,/mk_line,line_map=band_300_310,  
ion='broadband',wmin=300,wmax=310
```

We set ion='broadband', which uses an isothermal calculation over 165-550 Å with the keyword ergs set, and includes (as with the previous isothermal call over 165-550 Å in photon units, used to calculate dem_map) all the emissions because sngl is not set in the coded isothermal call.

The next section contains an explanation of the file infile.list in the Solar Soft distribution.

Application of the DEM tool to solar EUV irradiances

The DEM map technique has been used in several previous papers, including modeling of the Fe XIV 5303 Å coronagraph green line observations from Sacramento Peak Observatory (Cook, Newmark, and Altrock, 2005), comparisons between EIT and SUMER observations from SOHO (Brosius et al., 2002), and modeling of the full sky He II 304 Å flux for application to analysis of observations from the GAS experiment on the Ulysses spacecraft (Auchere et al., 2005a, 2005b, 2005c).

This section is adapted from the texts of an earlier paper, and a proposal to NASA, on comparison of the EUV irradiance observed by the SEM instrument on SOHO with a synthetic model irradiance. We have included in our Solar Soft directory the file infile.list which lists the GSFC archive filenames of the four daily EIT images which we have used in the work described below. This work illustrates types of analysis which can be performed using our DEM tool:

Active regions rotating across the disk modulate the solar radiative output on a 27 day timescale, while over the 11-year solar activity cycle timescale the full-disk brightness varies with activity level as the fractional area of active regions increases. The brightness varies more strongly for emissions from higher-temperature plasmas, because of the increasing contrast with temperature of active regions to quiet regions on the surface. From space the Sun can be viewed at EUV wavelengths in a variety of emission lines spanning a range of emitting temperatures in the solar transition region and corona. Some of these, such as the He II 304 Å emission line, are significant to the physics of the upper terrestrial atmosphere. The EUV range is important for the terrestrial ionosphere, where it is the dominant ionizing flux at certain levels, and controls the dynamics of the thermosphere (Meier, 1991). He II 304 Å is also an important contributor to the solar flux at wavelengths controlling photoionization of neutral H and He atoms in the heliosphere. The solar EUV flux and its variability impacts a range of phenomena of physical interest.

We have modeled irradiances over 1996-2005, which covers the solar activity cycle from the previous cycle minimum epoch, to well past the cycle 23 maximum. For this period an accurate EIT absolute calibration is available.

We compute a DEM map for each day using four EIT images exposed closely together in time (20 minutes). From the daily DEM map we then calculate daily synthetic 10 Å band intensity images over 170-550 Å. Figure 1, from Newmark, Cook, and McMullin (2008), illustrates daily synthetic images for the two days 10 February 1997, a period of low solar activity level, and 3 January 2002, a period of higher activity, in solar cycle 23. For each day the integrated 260-340 Å intensity image and also the pure He II 304 Å line intensity image is illustrated. These two days are marked on the SEM irradiance history plot of Figure 2 below.

The intensity image is converted to the equivalent flux at 1 A.U., or the irradiance F , where $F = \pi \langle I \rangle / (1 \text{ A.U.} / R)^2$, where $\langle I \rangle$ is the average intensity out to radius R . Coronal lines can have significant off-limb emission, and we include intensities out to 1.3 R_{\odot} , which captures the great majority of off-limb emission, while not extending into low signal-to-noise areas of the EIT images. The EIT fluxes are observed at the location of the SOHO spacecraft, the Lagrangian Sun

-Earth L1 point. Using the spacecraft data files, this flux is converted to a standard 1 A.U. flux. Because the spacecraft orbital path can extend slightly above or below the ecliptic plane by about 0.01 A.U., this flux is not identically the irradiance (flux toward Earth at 1 A.U.), but we still refer to it as the irradiance. More detail is given in Newmark, Cook, and McMullin (2008).

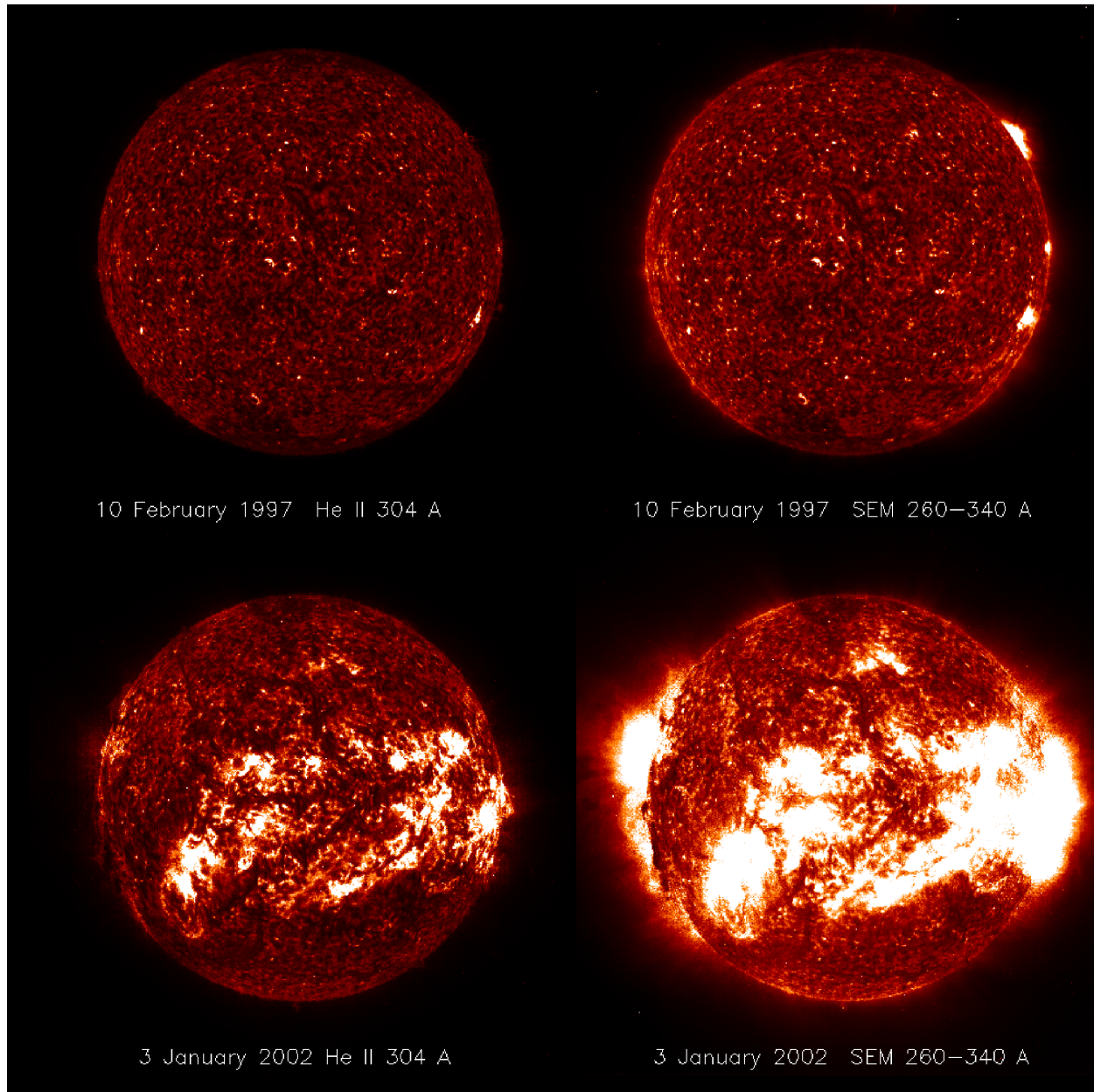


Fig. 1. Model synthetic images of the 260-340 Å and the pure He II 304 Å intensities for 10 February 1997 and 3 January 2002.

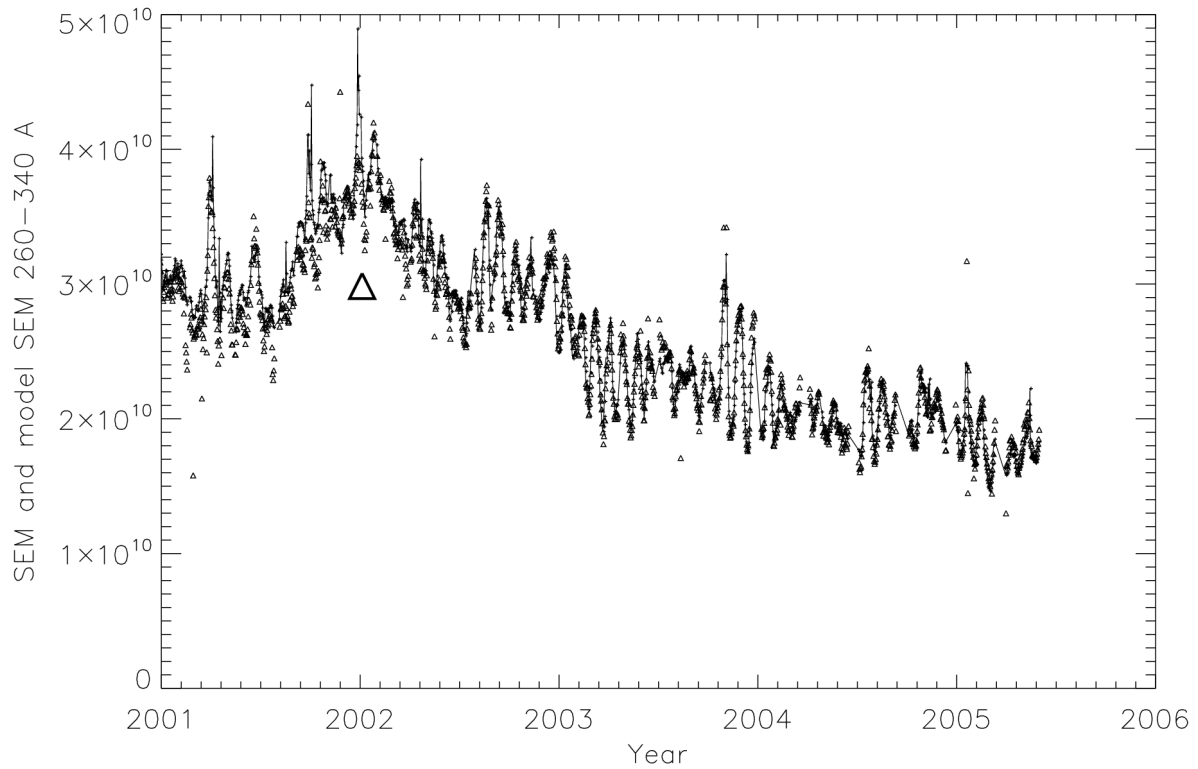
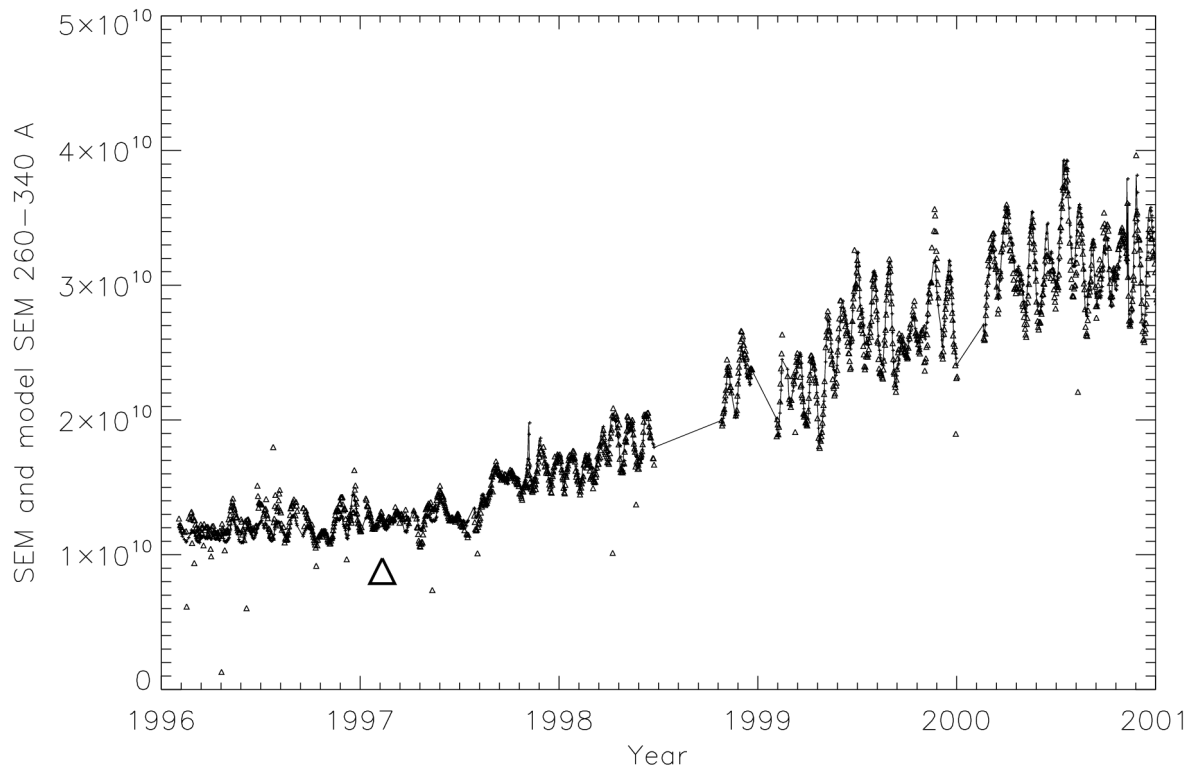


Fig. 2. Histories over 1996-2005 of the SEM 260-340 Å observed and model irradiances. SEM observations: + joined by line; SEM model: triangle. The two days of differing activity levels illustrated in Figure 1 are marked by triangular pointers from below.

Newmark, Cook, and McMullin (2008) compared model irradiances to the observed SOHO/SEM 260-340 Å irradiances (see Judge et al. 1998) over 1996-2005, finding little systematic long-term change in the fractional systematic error (Model/SEM) ~ 0.98 , and 19% scatter (3σ). Figure 2 illustrates from this paper the time histories over 1996-2005 of the 260-340 Å observed SEM and our model irradiances. The SEM monitor should have a particularly accurate long term absolute calibration, from a pre-launch laboratory calibration and several tracking comparisons with calibration rocket underflights over 1996-2006 (Judge, McMullin, and Ogawa 1999; McMullin et al. 2002). The analysis of the error in the SEM irradiances by McMullin et al. (2002) gives a 3σ fractional error of $\pm 30\%$. Newmark, Cook, and McMullin (2008) give the error in the model SEM irradiances as $\pm 32\%$. The good agreement, within the errors of both the SEM and EIT calibrations, suggests that the calibration of the EIT observations (Newmark et al. 2000) behind the DEM maps is accurate. While the actual strong numerical agreement may be fortuitous considering the error estimate for both the observations and the model results, it is still satisfying to be this close, instead of at the extremes of the error overlaps, even though this too would represent agreement. The excellent short term rotational time scale agreement is a strong indicator of the relative accuracy of the model.

We have already extended our wavelength coverage to 170-550 Å, and potentially can model additional wavelengths. We discuss the wavelength range that we can model in terms of the contributions to the solar EUV spectrum of emissions from differing temperature regions of the solar atmosphere, and of the range of applicability of our DEM map method. Our technique is limited to modeling optically thin emissions from plasmas over the range of temperatures $\log T = 4.6-6.5$ that contribute to the images from the four EIT channels defining the DEM map. This is a temperature, not wavelength, limitation, and Cook, Newmark, and Altrock (2005), for example, have compared a DEM map model Fe XIV 5303 Å green line index with the Sacramento Peak coronagraph green line observations at visible wavelengths. EUV irradiances over 170-550 Å arise from this EIT temperature sensitivity range, but to shorter wavelengths below 170 Å emissions will eventually start to arise from plasmas hotter than $\log T = 6.5$.

In Figure 3 we illustrate the temperature contribution functions $dI/d\log T$ of the two wavelength bands 110-120 Å and 170-180 Å for the representative CHIANTI quiet and active region DEM curves. The integrated area under each curve is the total emission intensity in the band (not the irradiance), plotted logarithmically. The CHIANTI active region DEM extends to $\log T = 6.8$ and will produce an intensity contribution at higher temperatures if hotter plasmas contribute emission to an individual band. Figure 3 demonstrates that the 170-180 Å band can be realistically modeled by our DEM map technique, while the 110-120 Å band will have contributions from plasmas hotter than we treat. Flare lines at any wavelength cannot be modeled.

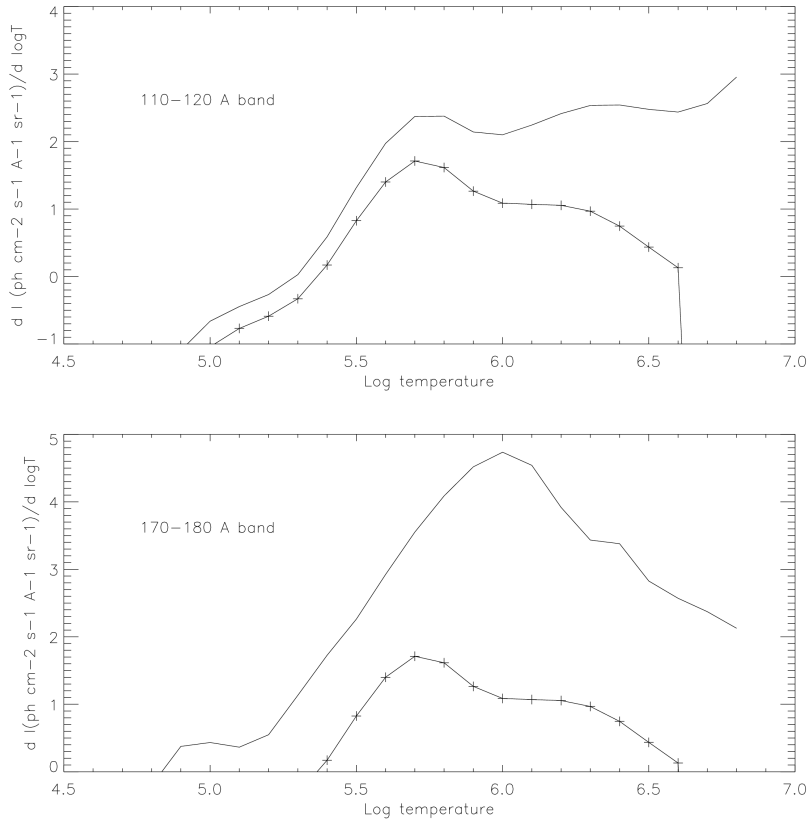


Fig. 3. Temperature contribution functions for the 110-120 Å and 170-180 Å bands, using the CHIANTI quiet (line with +) and active region (line) DEM curves. Intensity is plotted logarithmically.

To longer wavelengths above optically thick Lyman alpha 1215 Å an optically thick continuum and chromospheric emission lines, together with optically thin transition region and a few coronal emission lines, contribute emissions. Above 1680 Å the Fraunhofer spectrum begins. The wavelength range past Lyman alpha cannot be modeled by a DEM technique except for the individual optically thin transition region and coronal emission lines present. Even to shorter wavelengths several strong optically thick emission lines occur, especially He II 304 Å, but also He I 584 Å and H I Lyman beta 1025 Å. We use an observationally determined multiplier to treat the pure He II 304 Å line separately within the EIT 304 Å channel, and discussed this treatment in Newmark, Cook, and McMullin (2008). We need to do this to utilize the EIT 304 Å channel to tie down the cooler end of the DEM curve, but do not intend to push on similarly to treat other optically thick lines. Finally, above 750 Å the hydrogen Lyman continuum, up to the photoionization edge at 911 Å, is increasingly important. Although we have added a sketchy treatment for continua emitted down to $\log T = 4.0$, we have not yet made sufficient comparisons with available observations to trust this at longer wavelengths where the cool continuum is a meaningful contributor to the irradiance. We will quantitatively study extending our modeling to additional EUV wavelengths. We do now have confidence in applying our DEM map technique

over at least the 170-550 Å range. We report our results in 10 Å bins, but can calculate any wavelength resolution, including individual emission lines, to a resolution where assumptions on individual line profiles become critical for accuracy.

We have included our approximate treatment for continua formed over $\log T = 4.0-4.6$ by extending the DEM curve to cooler temperatures than sampled by the EIT channels. We have always included continua arising from the temperature sensitivity range directly sampled by EIT; this is just a switch in the CHIANTI program the user sets, and makes little numerical difference over our standard temperature range. We added the extension down to $\log T = 4.0$ in preparation to better model the irradiances longward of the EIT channels. When we use this treatment only over 170-550 Å, in this range it is numerically still a small contribution.

Our DEM map technique produces synthetic daily images, and allows the determination of the irradiance contribution arising from individual structural features, and the separate calculation of an on-disk and off-disk irradiance component. The off-disk component becomes increasingly significant for hotter coronal emissions, and can be appreciated in the synthetic images shown in Figure 1. This irradiance segmentation is also useful for modeling the projection of the irradiance viewed in the Earth direction to other, non-ecliptic, viewing directions. While the disk component can be obtained from a Carrington format map, projected to any viewing angle (see Auchere et al. 2005a, 2005b, 2005c), the off-disk component cannot be directly projected (short of tomographic reconstruction) because of the infinite line-of-sight beyond the limb.

We illustrate in Figure 4 a plot of the on-disk and off-disk irradiance histories at top, and at bottom the statistical relationship between the on-disk and off-disk components, for the 270-280 Å band. We have obtained this type of relationship over the entire 170-550 Å range for each 10 Å band. This division is also interesting because of the different behavior of the two components with solar rotation. The disk component irradiance is modulated by the passage across the disk of bright active regions on a 27 day timescale. The off-disk component is also modulated by bright active regions, but by those at the east and west limbs, and is frequently modulated on a 13 day timescale 90° out of phase with the disk component, because the line-of-sight is not limited by an opaque disk (earlier discussed for the Fe XIV 5303 Å index in Cook, Newmark, and Altrock 2005).

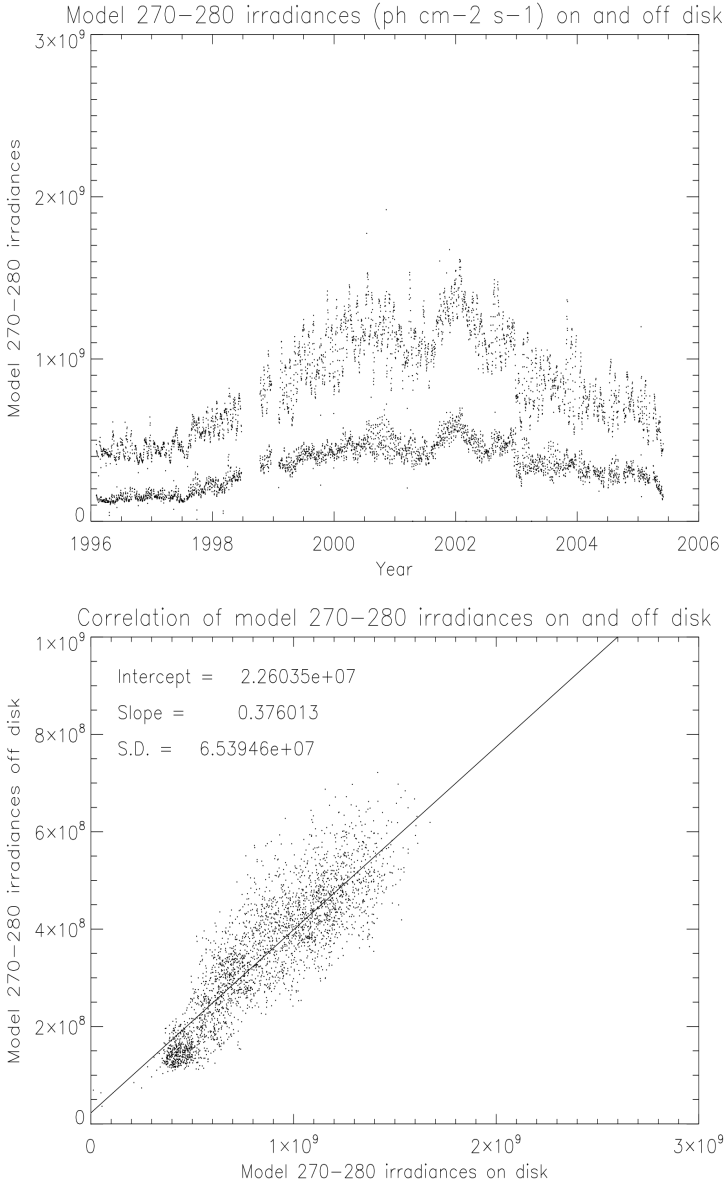


Fig. 4. Top: on-disk and off-disk irradiance histories for the 270-280 Å band. Bottom: correlation of the on-disk and off-disk irradiances.

References

- Auchere, F., Cook, J. W., Newmark, J. S., McMullin, D. R., von Steiger, R., and Witte, M. 2005a, *Advances Space Res.*, 35, 388
- Auchere, F., Cook, J. W., Newmark, J. S., McMullin, D. R., von Steiger, R., and Witte, M. 2005b, *Ap. J.*, 625, 1036
- Auchere, F., McMullin, D.R., Cook, J.W., Newmark, J.S., Von Steiger, R., and Witte, M. 2005c, *Proc. Solar Wind 11 - SOHO 16*, ESA SP-592, 327
- Brosius, Jeffrey W., Landi, Enrico, Cook, John W., Newmark, Jeffrey S., Gopalswamy, N., and Larra, Alejandro 2002, *Ap. J.*, 574, 453
- Cook, J. W., Newmark, J. S., and Altrock, R. C. 2005, *Ap. J.*, 633, 518
- Cook, J.W., Newmark, J.S., and Moses, J.D. 1999, in *Proceedings of the 8th SOHO Workshop: Plasma Dynamics and Diagnostics in the Solar Transition Region and Corona*, ed. J.-C. Vial and B. Kaldeich-Schumann (Noordwijk: ESA SP-446), 241
- Delaboudiniere, J.-P., and 27 co-authors 1995, *Solar Phys.*, 162, 291
- Dere, K.P., Landi, E., Mason, H.E., Monsignori Fossi, B.C., and Young, P.R. 1997, *A&A Suppl.*, 125, 149
- Feldman, U., Mandelbaum, P., Seely, J.F., Doschek, G.A., and Gursky, H. 1992, *Ap. J. Suppl.*, 81, 387
- Howard, R.A., Moses, J.D., Socker, D.G., Dere, K.P., Cook, J.W., and the SECCHI Consortium 2002, *Adv. Space Res.*, 29, 2017
- Judge, D.L., McMullin, D.R., and Ogawa, H.S. 1999, *J.G.R.*, 104, 28321
- Judge, D.L., McMullin, D.R., Ogawa, H.S., Hovestadt, D., Klecker, B., Hilchenbach, M., Mobius, E., Canfield, L.R., Vest, R.E., Watts, R., Tarrío, C., Kühne, M., and P. Wurz, P. 1998, *Solar Phys.*, 177, 161
- Mazzotta, P., Mazzitelli, G., Colafrancesco, S., and Vittorio, N. 1998, *A&A Suppl.*, 133, 403
- Meier, R.R. 1991, *Space Sci. Rev.*, 58, 1
- McMullin, D. R., Judge, D. L., Hilchenbach, M., Ipavich, F., Bochsler, P., Wurz, P., Burgi, A., Thompson, W. T., and Newmark, J. S. 2002, in *The Radiometric Calibration of SOHO*, ed. A. Pauluhn, M.C.E. Huber, and R. von Steiger (Bern: International Space Science Institute SR-002), 135

Newmark, J.S., Cook, J.W., and McMullin, D.R. 2008. This paper can be viewed at <http://sungrazer.nrl.navy.mil/docs/sem.ps>.

Newmark, J.S., Moses, J.D., Cook, J.W., Delaboudiniere, J.-P., Song, X., Carabetian, C., Bougnet, M., Brunaud, J., Defise, J.-M., Clette, F., and Hochedez, J.-F. 2000, SPIE, 4139, 328